THE ASTROPHYSICAL JOURNAL, 481:587–593, 1997 June 1

POTENTIAL MEASUREMENT OF THE LUMINOSITY FUNCTION OF 158 MICRON [C II] AT HIGH REDSHIFTS: A TEST OF GALAXY FORMATION MODELS

ANTONY A. STARK
Smithsonian Astrophysical Observatory; 60 Garden Street, MS 78, Cambridge, MA 02138; aas@cfa.harvard.edu
Received 1996 March 18; accepted 1996 December 24

ABSTRACT

Galaxy formation scenarios predict a burst of star formation in normal galaxies at a redshift between $z \sim 2$ and $z \sim 6$ (e.g., Katz & Gunn 1991); such a starburst may be accompanied by a significant brightening of the $\lambda = 158$ μm line of C^+. Galaxies that will evolve to a total luminosity $L^* = 5 \times 10^{10}\ L_\odot$ in the current era are considered at various redshifts. When the C^+ luminosity is evolved in accordance with a starburst scenario, the expected spectral line antenna temperature at the focus of a 10 m telescope is about 2 mK for galaxy models at redshifts up to that at which the starburst occurs. Such a spectral line is detectable with current submillimeter wavelength instrumentation at good submillimeter-wave sites like the South Pole. If the telescope were equipped with an array receiver and wide-bandwidth spectrometers (100 channels distributed over 5 GHz), a "blank sky" survey for such objects would likely detect several hundred during a winter of observation. The number and distribution of detections would provide a sensitive test of galaxy formation models, even if protogalaxies are shrouded in dust and faint at near-infrared wavelengths. Most of the energy released in the collapse of protogalaxies and the first generations of star formation may appear at Earth as submillimeter-wave radiation; testing this hypothesis will necessarily require submillimeter-wave observations.

Subject headings: early universe — galaxies: formation — infrared: galaxies — radio lines: galaxies

1. INTRODUCTION

Among all current theories of galaxy formation, cold dark matter (CDM) scenarios (Katz, Hernquist, & Weinberg 1992) have the greatest consistency with observation and the greatest explanatory power. CDM scenarios tend to form most large galaxies fairly late ($z \sim 2$) in an energetic burst of star formation (Baron & White 1987; Katz & Gunn 1991; Katz 1992), with the occasional rare object formed as early as $z \sim 8$ (Katz et al. 1994). The confrontation of theory with observation has shown areas of possible discrepancy, relating to the timing and intensity of galaxy formation. Cosmic microwave background observations ($z > 1000$) (White, Scott, & Silk 1994) show only weak fluctuations that may evolve into galaxies. Quasars, which are almost certainly a relatively rare phenomenon in active galactic nuclei, are first observed at $z \sim 5$ (Schmidt, Schneider, & Gunn 1989). In the present era, there are few objects that seem to be galaxies in formation, and there are many galaxies with star formation activity that, extrapolated back in time at the current rate, is insufficient to produce the quantity of stars or metals present. Thus, sometime after $z \sim 1000$, but before $z \sim 1$, galaxies formed and had relatively high star formation rates. A more precise determination of the era of galaxy formation is the focus of current observational effort at visual and near-infrared wavelengths. Guhathakurta, Tyson, & Majewski (1990), Steidel et al. (1996), and Yee et al. (1996) have detected galaxies at $z \sim 3$ that show relatively high rates of star formation. The density of these objects is high: they are a significant fraction, perhaps a majority, of all galaxies at that redshift and may be the first direct observational evidence of a protogalactic age.

Statistically reliable measurement of galaxy formation activity at visual and near-infrared wavelengths is troubled by the presence or possible presence of dust. Charlot & Fall (1993) have argued that there may be only a brief period at the beginning of star formation between the generation of significant Lyα emission and the shrouding of that light by dust. Ostriker & Cowie (1981) suggest that all objects at $z > 3$ may be significantly attenuated by dust. Steidel et al. (1996) argue that the galaxies they observed at $3.5 > z > 3.0$ are relatively free of dust, but if that is the case, then why is Lyα weak or absent in some of their sample? It is possible that they are seeing only the very beginnings of a starburst and that the bulk of the luminosity occurs later under an obscuring cover of dust. Protogalaxies may resemble the ultraluminous infrared galaxies seen at low redshift, in which case their average internal visual extinction would be $A(V) \approx 50$–500 mag (Lutz et al. 1996), making the redshifted galaxy unobservable at visual and even near-infrared wavelengths. The resolution of this difficulty may lie, as it does in studies of star formation in the Milky Way, at much longer wavelengths.

The $^2P_{3/2} \rightarrow {}^2P_{1/2}$ line of C^+ at $\lambda = 158$ μm is the brightest emission line in the spectrum of most galaxies. From the radio to X-ray, the wavelength of highest flux density in a galaxian spectrum is usually the peak of this line; as much as 0.5% of the total luminosity of a galaxy can be emitted in the single spectral line (Stacey et al. 1991; Wright et al. 1991). At redshifts of $z \simeq 1$ to $z \simeq 6$, the line is shifted into the submillimeter-wave band, wavelengths at which there are large telescopes and excellent detectors. At these wavelengths, essentially all lines of sight are optically thin out to $z > 30$, and the number of interfering foreground sources is small. It has therefore been proposed (e.g., Petrosian, Bahcall, & Salpeter 1969; Loeb 1993) that this line could be detected from galaxies at high redshift and could be used to observe protogalaxies.

The purpose of this paper is to present calculations of the expected brightness of the C^+ line at high redshift and to evaluate the possibility of using it in "blank sky" and directed studies of high-redshift galaxies, in the context of current submillimeter-wave technology applied at the best available observatory site. A hypothetical luminosity func-

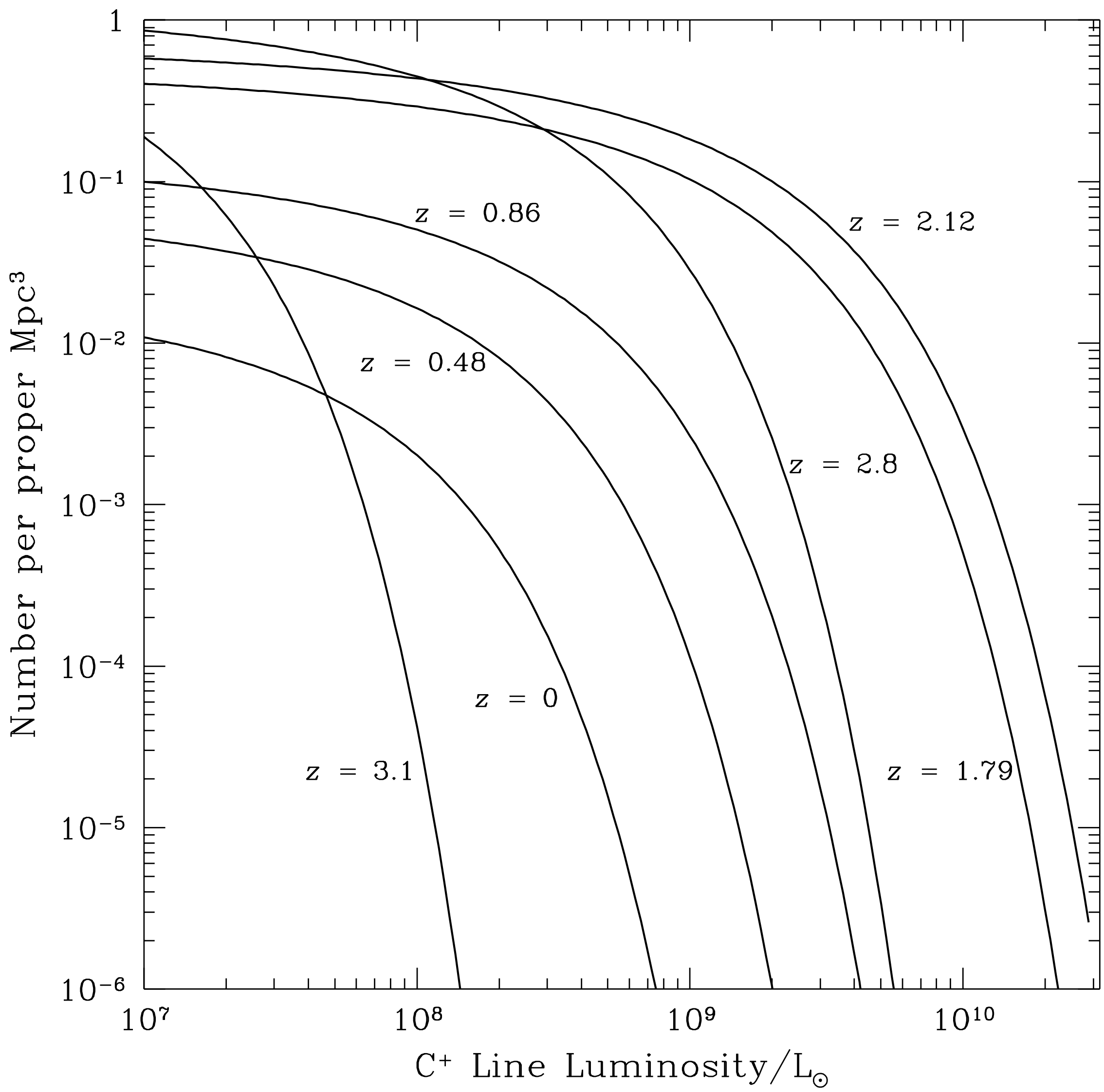

FIG. 1.—Integral form of a hypothetical C$^+$ luminosity function for galaxies, as described by eqs. (1) and (2). The abscissa is $^2P_{3/2} \rightarrow {}^2P_{1/2}$ C$^+$ line luminosity, in solar luminosities. The ordinate is the number density of galaxies whose luminosity exceeds that value. The luminosity function is shown for seven eras, labeled by redshift z. Number density is for a proper volume and no mergers, so the total number of galaxies varies as $(1 + z)^3$.

tion for the C$^+$ line in galaxies is presented in § 2. The relation between luminosity and observed brightness of high-redshift C$^+$ is calculated in § 3. The rates at which galaxies might be found in "blank sky" searches is discussed in § 4.

2. A HYPOTHETICAL C$^+$ LUMINOSITY FUNCTION FOR GALAXIES

What is the luminosity of the C$^+$ line in galaxies, and how luminous is it likely to be at high redshift? In summary of the observational data on C$^+$ in nearby galaxies, Stacey et al. (1991) have made three general statements: (1) C$^+$ luminosity is a measure of star formation activity; (2) C$^+$ luminosity is roughly proportional to total galactic luminosity, $L_{C^+} \simeq 0.002 L_{\rm gal}$, for spiral and irregular galaxies; and (3) C$^+$ luminosity is not strongly dependent on metallicity. The implication is that, roughly speaking, the C$^+$ luminosity function of nearby galaxies has the same form as the Schechter (1976) function for galactic luminosity, except that the C$^+$ line constitutes only 1/500th of the total. If this is assumed to hold for high-redshift galaxies as well, then theoretical models of galaxy formation that calculate expected galactic luminosities can be used to frame a hypothesis about C$^+$ line luminosities at all redshifts. Take $l_{C^+} \equiv L_{C^+}/L_{\rm gal} \simeq 0.002$, and following Schechter (1976), the C$^+$ line luminosity function of the form

$$\phi(L_{C^+}) dL_{C^+} = \phi^*(z) \left[\frac{L_{C^+}}{L^*_{C^+}(z)}\right]^\alpha \exp\left[-\frac{L_{C^+}}{L^*_{C^+}(z)}\right] d\left[\frac{L_{C^+}}{L^*_{C^+}(z)}\right], \quad (1)$$

where $\alpha = -0.7$, $\phi^*(z) = 8 \times 10^{-3}\, h_{75}^3 (1 + z)^3$ Mpc^{-3} ($h_{75} \equiv H_0/75$ km s^{-1} Mpc^{-1}), and $L_0^* = 5 \times 10^{10}\, h_{75}^{-2}\, L_\odot$ (Lin et al. 1996). In CDM galaxy formation models (Katz 1992), galaxies peak in luminosity at a redshift $z_b \sim 2.2$ and decay afterward at a roughly exponential rate:

$$L^*_{C^+}(z) = l_{C^+} L^*(z) = l_{C^+} L_0^* \exp\left\{m_b\left[\frac{\beta z_b^\beta z - z_b z^\beta}{(\beta - 1) z_b^{\beta+1}}\right]\right\}. \quad (2)$$

Larger β describes a starburst that turns on more rapidly,

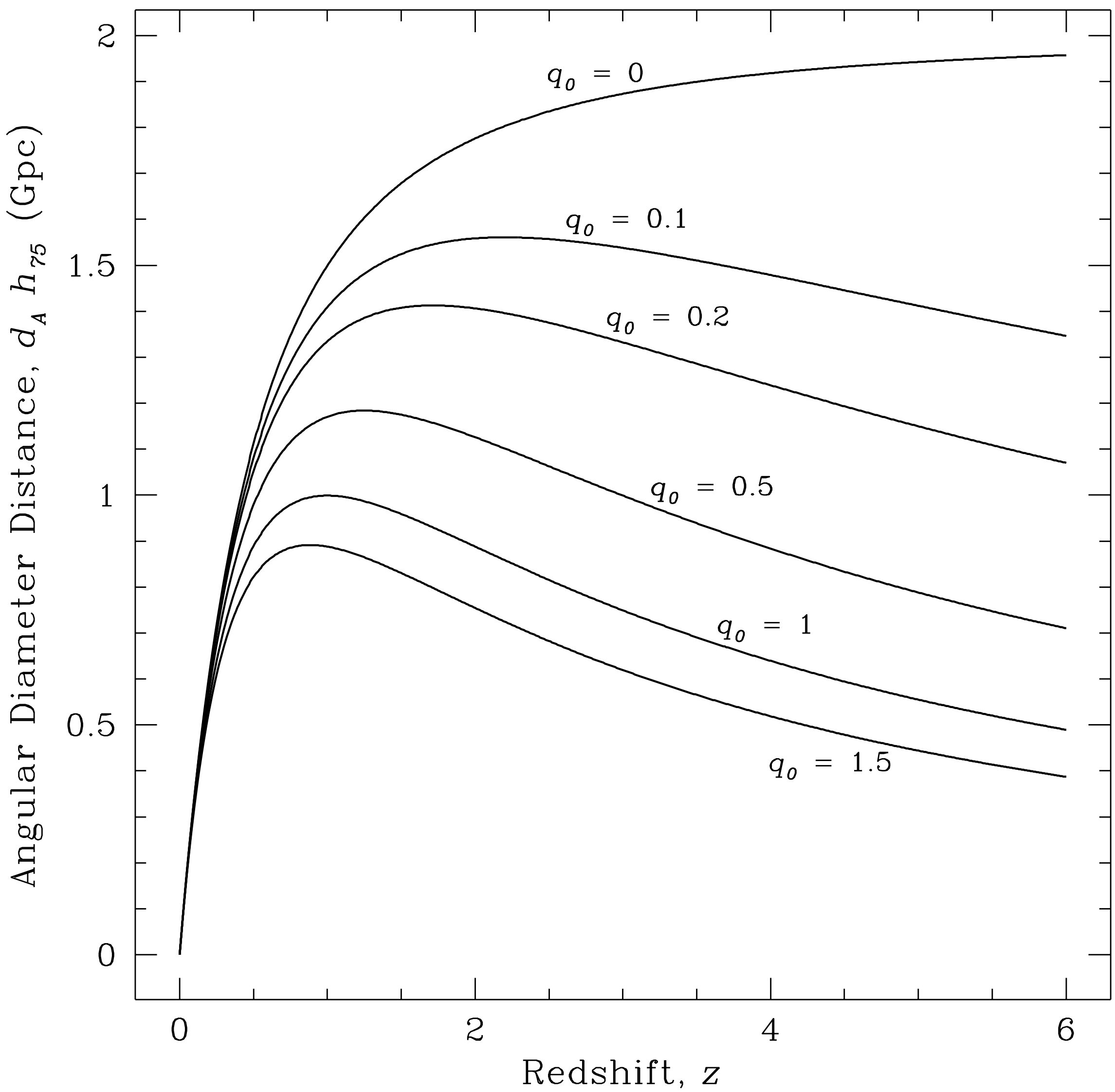

FIG. 2.—Angular diameter distance d_A h_{75} as a function of redshift for $q_0 = 0$, 0.1, 0.2, 1/2, 1, and 3/2. See eq. (5).

and the intensity of the burst is $L_b = L_0^* \exp(m_b)$. These equations imply that all galaxies form at the same time, do not merge, and go through a starburst at the same redshift, z_b. This may not be the case (De Araujo & Opher 1994), but the argument below requires only that the estimates of $\phi(L_{C^+})$ and $L_{C^+}(z)$ be correct for most of the bright (i.e., L^*) galaxies.

Figure 1 is a plot of $\int_L^\infty \phi(L_{C^+}) dL_{C^+}$ for various redshifts, where the starburst parameters $\beta = 8$, $m_b = 3.2$, and $z_b = 2.2$ are suggested by the work of Katz (1992). These values are adopted below, to allow definite predictions about the detection of such galaxies. Figure 1 shows the number density of galaxies with C^+ line luminosities greater than a given value. Note that the density of all galaxies increases with redshift because of universal expansion and that all galaxies are more luminous near the redshift of the starburst. Also considered below is the case $\beta = 8$, $m_b = 3.2$, and $z_b = 4.4$, as an example of a starburst at an earlier era.

3. THE LUMINOSITY-REDSHIFT RELATION

The Friedman-Robertson-Walker metric can be used to describe the spacetime geometry of a homogeneous and isotropic universe:

$$d\tau^2 = dt^2 - \frac{R^2(t)}{c^2}\left(\frac{dr^2}{1-kr^2} + r^2 d\theta^2 + r^2 \sin^2\theta\, d\phi^2\right), \quad (3)$$

where r, θ, ϕ, and t are coordinates, $k = \pm 1$ or 0, and $R(t)$ is a cosmological scale factor that contains all the dynamics. The spatial coordinates, r, θ, and ϕ, are comoving, so that an observer with zero peculiar velocity (e.g., on a galaxy) has these coordinates fixed for all time. The time coordinate, t, is the clock time of all such comoving observers.

A photon leaves a distant galaxy at coordinate (t_1, r_1, θ_1, ϕ_1) and travels along a trajectory $\theta_1 =$ constant, $\phi_1 =$ constant, until it arrives at $r = 0$ at time t_0 and is detected by a telescope. The frequency of detection, ν_0, is related to the frequency of emission, ν_1, by

$$\frac{1}{1+z} \equiv \frac{\nu_0}{\nu_1} = \frac{\lambda_1}{\lambda_0} = \frac{R(t_1)}{R(t_0)}. \quad (4)$$

(Note that the subscript 0 refers to the observed line and that the subscript 1 refers to the rest frame of the distant galaxy.) If l is the physical size of the distant galaxy, say 10 kpc, and it subtends an angle δ at Earth, then the angular diameter distance is

$$d_A \equiv \frac{l}{\delta} = R(t_1)r_1 = \frac{c}{H_0}\left[\frac{zq_0 + (q_0 - 1)(\sqrt{2q_0 z + 1} - 1)}{q_0^2(1+z)^2}\right], \tag{5}$$

where H_0 is the Hubble constant at time t_0, and q_0 is the deceleration parameter at time t_0 (Mattig 1958). Figure 2 is a plot of $d_A\, h_{75}$ as a function of z, for $q_0 = 0$, 1/2, 1, and 3/2, and it shows that $d_A \sim 1$ Gpc h_{75}^{-1} for $0.3 < z < 6$ and for all reasonable big bang cosmologies.

If the luminosity of the C^+ line at the source is L_{C^+}, then the received flux is

$$F_{C^+} = \frac{L_{C^+}}{4\pi}\left[\frac{R(t_1)}{r_1 R^2(t_0)}\right]^2 = \frac{L_{C^+}}{4\pi d_A^2(1+z)^4} \tag{6}$$

(see Weinberg 1972, pp. 485 and 504). This flux will be distributed in frequency over the width of the spectral line, which is spread out by the rotation of the galaxy. The fractional bandwidth of the line, $\Delta v/v$, is independent of redshift. The observed galaxy may be face-on or edge-on, so $\Delta v/v = \Delta v/c \sim 10^{-3}$ to 10^{-4}. Observed with an antenna of diameter D and aperture efficiency η ($\sim$0.8), the antenna temperature of the line is then

$$T_A^* = \frac{1}{2k}\left(\eta\,\frac{\pi}{4}\,D^2\right)\frac{F_{C^+}}{\Delta v_0} = \frac{\eta D^2 L_{C^+} v_0^4}{32 k v_1^4 d_A^2 \Delta v_0}$$
$$= 1\ \text{mK}\left[\frac{\eta D^2}{(10\ \text{m})^2}\right]\left(\frac{L_{C^+}}{10^9\ L_\odot}\right)\left(\frac{v_0}{500\ \text{GHz}}\right)^3$$
$$\times\left(\frac{1\ \text{Gpc}}{d_A}\right)^2\left(\frac{250\ \text{km s}^{-1}}{\Delta v}\right), \tag{7}$$

for zero atmospheric absorption.

4. DETECTABILITY USING GROUND-BASED TELESCOPES

The line brightnesses indicated by equation (7) are faint, but not impossibly faint. Consider a protogalaxy that will evolve into a galaxy with total luminosity L^* in the current era: such a galaxy will be called "an L_0^* galaxy," regardless of the redshift at which it is observed. Table 1 shows the observing time needed to detect an L_0^* galaxy (whose C^+ luminosity is given by eq. [2]) in the submillimeter-wave atmospheric windows, with a 10 m antenna at the South Pole during good winter weather (Bally 1989; Chamberlin, Lane, & Stark 1997), using currently existing submillimeter-wave receivers, for starburst models at the two eras $z_b = 2.2$ and $z_b = 4.4$, as discussed in § 2. The frequencies in this table are chosen to be near the peak of the atmospheric windows; it is easier to detect the line at these redshifts than at others. The equivalent system temperature,

$$T_{\text{sys}}^* = [T_{\text{receiver}} + \eta_{\text{mb}}\, T_{\text{atmosphere}}(1 - e^{-\tau_0 A}) + (1 - \eta_{\text{mb}})T_{\text{ambient}}]\,\frac{e^{\tau_0 A}}{g\eta_{\text{mb}}},$$

is the system temperature that satisfies the atmospheric-corrected radiometer equation

$$T_{\text{rms}}^* = \frac{T_{\text{sys}}^*}{\sqrt{t\,\Delta v}},$$

where $\eta_{\text{mb}} \sim 0.9$ is the main-beam efficiency, g is the relative sideband gain, τ_0 is the zenith atmospheric opacity, and T_{rms}^* is the noise in the atmospheric-corrected data. Table 1 shows that the C^+ line can be detected in less than 1 hr at redshifts near z_b. Rapid development of receivers at frequencies near 1 THz (Carlstrom & Zmuidzinas 1996) will likely reduce the observing times for smaller redshift. For directed observations, in which the position and redshift of a bright, star-forming galaxy is known, the C^+ line should be detectable.

Visual wavelength detection surveys for high-redshift galaxies may be incomplete because of the presence of dust. It is therefore desirable to carry out "blank sky" searches, in which neither the position nor the redshift is known. What is the probability that a suitably bright galaxy will be within the beam of the telescope, at a redshift that falls within the spectrometer bandwidth? The submillimeter-wave receivers used for the calculation in Table 1 have relatively narrow instantaneous bandwidths, on the order of $\Delta v/v \sim 0.002$ to 0.02. The proper volume observed by the telescope in any single observation can therefore be approximated as a cylinder at a single epoch. The diameter of the cylinder is approximately $d_A\,\delta_{\text{beam}}$, where

$$\delta_{\text{beam}} \simeq 20''\left(\frac{10\ \text{m}}{D}\right)\left(\frac{500\ \text{GHz}}{v_0}\right) \tag{8}$$

is the antenna beam size. If a galaxy is observed at redshift z, the coordinate time, t, at which the photons leave the galaxy is related to the redshift by $dt = -H_0^{-1}(1 + 2q_0 z)^{-1/2}(1+z)^{-2}\,dz$ (Weinberg 1972), so the proper length of the cylinder is given by

$$c\,\Delta t \simeq \frac{c}{H_0}\,\frac{1}{(1+z)\sqrt{1+2q_0 z}}\,\frac{\Delta v_0}{v_0}\,. \tag{9}$$

For the "just closed" case $q_0 = \frac{1}{2}$, this is particularly simple, and the proper volume that can be observed with a single beam and a single tuning of the receiver is then

$$V_{\text{prop}} \simeq \frac{\pi}{4}\,\delta_{\text{beam}}^2\, d_A^2\,\frac{c}{H_0}\,(1+z)^{-3/2}\,\frac{\Delta v_0}{v_0} = 0.05\ \text{Mpc}^3\ h_{75}^{-1}$$
$$\times\left(\frac{d_A}{1\ \text{Gpc}}\right)^2\left(\frac{10\ \text{m}}{D}\right)^2\left(\frac{500\ \text{GHz}}{v_0}\right)^{1.5}\left(\frac{\Delta v_0}{5\ \text{GHz}}\right). \tag{10}$$

This volume can be compared to the density of galaxies. Assuming no mergers, the proper density of L_0^* or brighter galaxies is $n \simeq 0.002\ \text{Mpc}^{-3}\ h_{75}^3(1+z)^3$, (Schechter 1976; Lin et al. 1996), so the expected number of bright galaxies in V_{prop} is

$$V_{\text{prop}}\, n \simeq 0.006\ h_{75}^2\left(\frac{d_A}{1\ \text{Gpc}}\right)^2\left(\frac{10\ \text{m}}{D}\right)^2$$
$$\times\left(\frac{500\ \text{GHz}}{v_0}\right)^{4.5}\left(\frac{\Delta v_0}{5\ \text{GHz}}\right). \tag{11}$$

Since $d_A \propto h_{75}^{-1}$, this quantity is independent of errors in the determination of the Hubble constant. An array receiver with 20 pixel elements and 5 GHz bandwidth at 500 GHz on a 10 m telescope would expect to cover one L_0^* galaxy for every six positions searched. Note that the expected number of galaxies per beam is a very strong function of redshift: the volume observed grows roughly as the 1.5 power of redshift, and the density of galaxies grows as the cube of redshift. The effect of this is shown in the "observing time per detec-

TABLE 1

OBSERVING TIME TO DETECT HIGH-z C^+ IN SUBMILLIMETER-WAVE ATMOSPHERIC WINDOWS

						$z_b = 2.2$			$z_b = 4.4$		
ν_0 (GHz) (1)	z (2)	Atmospheric Transmission (3)	T_{rec} DSB (K) (4)	References (5)	Equivalent T^*_{sys} (K) (6)	Expected Line Brightness (mK) (7)	Observing Time (hr) (8)	Observing Time per Detection for Array (hr) (9)	Expected Line Brightness (mK) (10)	Observing Time (hr) (11)	Observing Time per Detection for Array (hr) (12)
330	4.76	0.96	53	1	176	...	...	...	1.0	4.1	8.0
350	4.43	0.95	56	1	186	...	...	...	1.2	2.9	6.8
405	3.69	0.90	65	1	230	...	...	...	1.2	3.7	14
460	3.13	0.82	74	1	300	0.007	1.8×10^5	1.1×10^6	1.0	7.3	42
500	2.80	0.73	80	2	388	0.4	69	542	1.0	13.4	106
610	2.12	0.85	104	2	509	3.5	1.4	23	0.8	24	400
680	1.79	0.91	116	2	413	3.4	0.88	22	0.9	15	364
870	1.18	0.91	700	3	2032	2.7	27	1957	1.0	195	1.4×10^4
1020......	0.86	0.57	816	3	5544	2.7	170	2.6×10^4	1.3	717	1.1×10^5
1285......	0.48	0.63	3600	4	17800	4.1	614	3.8×10^5	2.7	1362	8.5×10^5
1350......	0.41	0.65	3800	4	17500	4.9	400	3.6×10^5	3.5	790	7.1×10^5
1500......	0.26	0.64	4200	4	21700	8.5	182	4.3×10^5	6.8	284	6.6×10^5

NOTES.—Atmospheric transmission is calculated for 1.1 air masses at the South Pole with 0.1 mm precipitable water vapor (Bally 1989; Chamberlin, Lane, & Stark 1997). T_{rec} values extrapolated from existing receivers reported by (1) Kooi et al. 1994, (2) Gaidis et al. 1996, (3) Bin et al. 1996, (4) Betz & Boreiko 1995, as shown in col. (5). Equivalent T^*_{sys} is the total single-sideband system temperature of an equivalently sensitive antenna above the atmosphere. The expected line brightness is the antenna temperature of an L^*_0 galaxy at the focus of a 10 m telescope (see eqs. [2] and [7]), using a simple galaxy formation model suggested by the work of Katz 1992. Observing time is the number of hours needed to make a 5 σ detection in each of five adjacent 50 km s^{-1} wide spectrometer channels. Observing time per detection is col. (8) divided by the number of L^*_0 galaxies covered by a single pointing of a 20 element array of receivers with 5 GHz bandwidth (see eq. [11]).

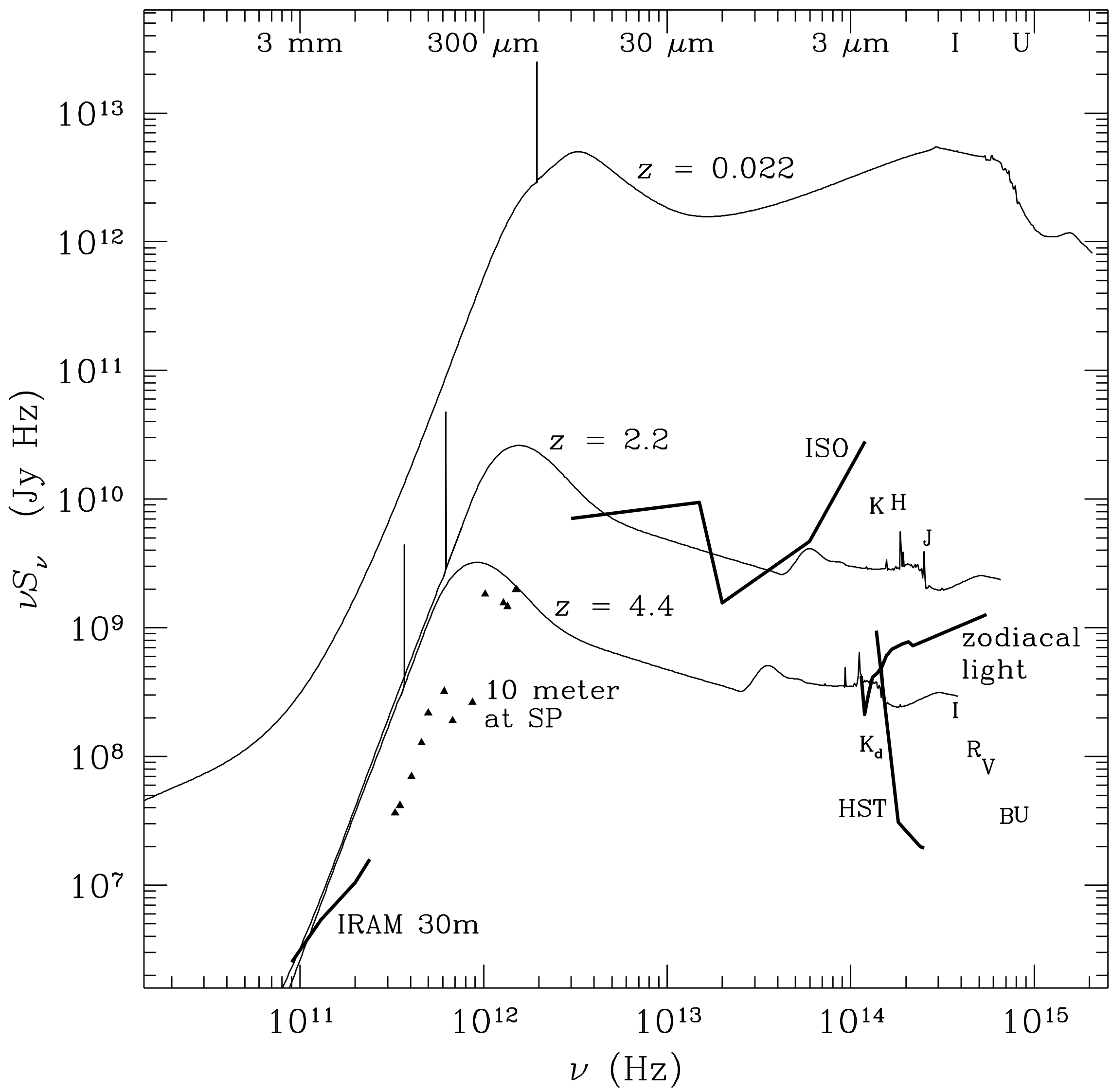

FIG. 3.—Normal galaxies at low and high redshift. The broadband galaxy spectrum labeled $z = 0.022$ has the luminosity and spectrum of M99, a normal L^* spiral. The spectra labeled $z = 2.2$ and $z = 4.4$ are models of the initial starburst in such a galaxy at two possible eras of the starburst, evolved in a standard CDM model (Katz 1992) with $h_{75} = 1$ and $q_0 = 1/2$. The 158 μm C^+ line is shown to scale; other lines are suppressed. The points KHJIRVBU are 1% of the sky brightness in 1 $arcsec^2$ at Mauna Kea (CFHT Observer's Handbook). The point K_d is 1% of the sky brightness in 1 $arcsec^2$ at the South Pole at $\lambda = 2.3$ μm. The curve labeled "zodiacal light" is the background sky brightness in 1 $arcsec^2$ measured by Noda et al. (1992). The curve labeled *HST* is the limiting sensitivity of the NICMOS on the *Hubble Space Telescope*. The curve labeled *ISO* is the sensitivity of the *Infrared Space Observatory* in 1 hr. The triangles show the continuum sensitivity in 1 hr of a 10 m South Pole telescope in the submillimeter-wave atmospheric windows. The curve labeled "IRAM 30 m" is the sensitivity in 1 hr of the 30 m telescope (Baars et al. 1987).

tion for array" columns of Table 1, which are the observing time needed to detect an L_0^* or brighter galaxy with a 20 element array of receivers with 5 GHz of intermediate-frequency bandwidth. The small volume that can be searched at low redshifts ($z < 1$) makes "blank sky" surveys impractical, even if receivers improve by an order of magnitude. At frequencies corresponding approximately to the era of the starburst, however, the detection rate is at least one per day, a rate which is practical and competitive with other methods of detecting high-redshift objects.

5. DISCUSSION

In the argument above, simple but plausible assumptions were used to calculate a hypothetical luminosity function for the $^2P_{3/2} \rightarrow {}^2P_{1/2}$ C^+ line in galaxies at high redshift and to show that this line is detectable even in a "blank sky" search. The instrument used in the calculation has the following properties: (1) a 10 m diameter antenna; (2) a 20 pixel array receiver operating at approximately 680 GHz; (3) 100 × 50 MHz spectrometer channels for each pixel in the array receiver; and (4) an observatory site at the South Pole. The instrument would search patches of sky approximately 1′ in size at low air mass near the south celestial pole, observing for a half-hour at each patch. Such a search would detect several hundred "normal" galaxies at $z \sim 3$ each austral winter and would provide a definitive test of galaxy formation hypotheses similar to the simple model in § 2. A practical observing program would probably be somewhat more complex. It might, for example, be more efficient to search for the redshifted 100 μm dust peak using bolometric photometer arrays at $\lambda = 200$, 350, and 450 μm and then verify the redshift of candidate objects with line receivers. The optimal instrument for detection of the redshifted C^+ line might prove to be a frequency-scanning bolometer array or grating spectrometer rather than the heterodyne receivers used for the calculations in Table 1.

Figure 3 illustrates the importance of submillimeter-wave observations to the study of protogalaxies. The broadband flux density of an L_0^* spiral galaxy is shown at low redshift and as a protogalaxy at two possible redshifts for the hypothetical starburst. The spectral distribution and luminosity of the low-redshift galaxy is that of M99 from the radio to the visible (Stark et al. 1989), matched onto a generic visible and ultraviolet spectrum for an Sbc galaxy (Coleman, Wu, & Weedman 1980). The spectral distribution of the high-redshift galaxies is that of M82 from the radio to the visible (Soifer, Houck, & Neugebauer 1987), matched onto a generic visible and ultraviolet spectrum for an Irr galaxy (Coleman et al. 1980). The bolometric luminosity of the high-redshift galaxies is $L_b = L_0^* \exp(m_b) = 24.5 L_0^*$ in both cases, and the flux is then calculated for $z = 2.2$ and $z = 4.4$ for $h_{75} = 1$ and $q_0 = \frac{1}{2}$. The two possible versions of the protogalaxy have a luminosity suggested by a CDM starburst model (Katz 1992), and this luminosity is assumed to have a spectral distribution like that of M82. Observations have shown that the size of the far-infrared flux peak varies widely from galaxy to galaxy and cannot be accurately predicted using observations at other wavelengths. Note that the protogalaxy curves fall within the sensitivity limit of the *Hubble Space Telescope* (*HST*), but only because of the extended ultraviolet brightness of the irregular galaxy spectrum. For the $z = 4.4$ case, *HST* can see only those photons that start out in the mid- and far-ultraviolet: this is essentially a sideshow to the main event, the flux of a few naked O stars that do not represent the stellar population as a whole. Only a small fraction of the bolometric luminosity appears in the visible; most of the luminosity appears in the submillimeter.

At a fixed submillimeter-wave frequency, galactic flux densities do not vary strongly with redshift. Galaxies have steep spectra in the submillimeter, $I(\nu) = C\nu^\gamma$, $\gamma \approx 2.7$, while as a function of redshift, $S_\nu \propto I[\nu(1+z)] d_A^{-2} (1+z)^{-3} = C\nu^\gamma d_A^{-2} (1+z)^{(\gamma-3)}$, where $d_A^{-2}(1+z)^{(\gamma-3)}$ is nearly independent of redshift. Depending on the precise spectral index γ and cosmological model, high-redshift galaxies can actually outshine their low-redshift cousins at submillimeter wavelengths, very different from the rapid dimming with redshift that occurs in the visible and infrared. Submillimeter-wave photometric colors may prove to be a powerful method for detecting high-redshift objects. For example, the only objects for which $S_{850\,\mathrm{GHz}}/S_{650\,\mathrm{GHz}} < 2$ are high-redshift galaxies with $z \gtrsim 4$.

The luminosity function presented in § 2 is highly simplified, and details such as the redshift and intensity of the starburst are likely to change with more refined models. Of critical importance to observations of protogalaxies are the role of dust in converting the energy of the starburst from visible light to submillimeter-wave radiation and the role of metallicity in determining the distribution of the submillimeter-wave power between line and continuum radiation. Near-infrared surveys are probably not capable of proving or disproving the hypothesis that most of the energy from the initial gravitational collapse of protogalaxies and the first burst of star formation is absorbed within the protogalaxy and reradiated at long wavelengths. Some form of submillimeter-wave search is needed. Whether that search should be done with narrowband or broadband techniques depends on the line-to-continuum ratio. Observations of nearby galaxies suggest that the line-to-continuum ratio may be high in low-metallicity systems, favoring a line search. One of the purposes of this paper has been to encourage more rigorous calculation of the C^+ luminosity implied by galaxy formation models; another is to promote the construction of a 10 m South Pole telescope.

I thank John Carlstrom, Merce Crosas, Charles Gammie, Adair Lane, Eve Ostriker, and Paul Schechter for discussions. Edward L. Wright made numerous helpful corrections and comments on the manuscript. This research was supported in part by the National Science Foundation (NSF) under a cooperative agreement with the Center for Astrophysical Research in Antarctica (CARA), grant NSF OPP89-20223. CARA is an NSF Science and Technology Center.

REFERENCES

Baars, J. W. M., Hooghoudt, B. G., Mezger, P. G., & de Jonge, M. J. 1987, A&A, 175, 319
Bally, J. 1989, in Astrophysics in Antarctica, ed. D. J. Mullan, M. A. Pomerantz, & T. Stanev (New York: AIP), 100
Baron, E., & White, S. D. M. 1987, ApJ, 322, 585
Betz, A. L., & Boreiko, R. T. 1995, in Proc. 6th Int. Symp. Space Terahertz Technology, ed. J. Zmuidzinas (Pasadena: California Inst. Tech.), 28
Bin, M., Gaidis, M. C., Zmuidzinas, J., Phillips, T. G., & LeDuc, H. G. 1996, Appl. Phys. Lett., 68, 1714
Carlstrom, J. E., & Zmuidzinas, J. 1996, in Reviews of Radio Science 1993–1996, ed. W. R. Stone (Oxford: Oxford Univ. Press), 839
Chamberlin, R., Lane, A. P., & Stark, A. A. 1997, ApJ, 476, 428
Charlot, S., & Fall, S. M. 1993, ApJ, 415, 580
Coleman, G. D., Wu, C.-C., & Weedman, D. W. 1980, ApJS, 43, 393
De Araujo, J. C. N., & Opher, R. 1994, ApJ, 437, 556
Gaidis, M. C., LeDuc, H. G., Miller, D., Bin, M., Stern, J. A., & Zmuidzinas, J. 1996, IEEE TMTT, 44, 1130
Guhathakurta, P., Tyson, J. A., & Majewski, S. R. 1990, ApJ, 357, L9
Katz, N. 1992, ApJ, 391, 502
Katz, N., & Gunn, J. E. 1991, ApJ, 377, 365
Katz, N., Hernquist, L., & Weinberg, D. H. 1992, ApJ, 399, L109
Katz, N., Quinn, T., Bertschinger, E., & Gelb, J. M. 1994, MNRAS, 270, L71
Kooi, J. W., Chan, M. S., Bumble, B., LeDuc, H. G., Schaffer, P. L., & Phillips, T. G. 1994, Int J. Infrared Millimeter Waves, 15, 783
Lin, H., Kirshner, R. P., Shectman, S. A., Landy, S. D., Oemler, A., Tucker, D. L., & Schechter, P. L. 1996, ApJ, 464, 60
Loeb, A. 1993, ApJ, 404, L37
Lutz, D., et al. 1996, A&A, 315, L137
Mattig, W. 1958, Astron. Nachr., 284, 109
Noda, M., Christov, V. V., Matsuhara, H., Matsumoto, T., Matsuura, S., Noguchi, K., Sato, S., & Murakami, H. 1992, ApJ, 391, 456
Ostriker, J. P., & Cowie, L. L. 1981, ApJ, 243, L127
Petrosian, V., Bahcall, J., & Salpeter, E. E. 1969, ApJ, 155, L57
Soifer, B. T., Houck, J. R., & Neugebauer, G. 1987, ARA&A, 25, 187
Schechter, P. 1976, ApJ, 203, 297
Schmidt, M., Schneider, D. P., & Gunn, J. E. 1989, AJ, 98, 1951
Stacey, G. J., Geis, N., Genzel, R., Lugten, J. B., Poglitsch, A., Sternberg, A., & Townes, C. H. 1991, ApJ, 373, 423
Stark, A. A., et al. 1989, ApJ, 337, 650
Steidel, C. C., Giavalisco, M., Pettini, M., Dickinson, M., & Adelberger, K. L. 1996, ApJ, 462, L17
Weinberg, S. 1972, Gravitation and Cosmology: Principles and Applications of the General Theory of Relativity (New York: Wiley)
White, M., Scott, D., & Silk, J. 1994, ARA&A, 32, 319
Wright, E. L., et al. 1991, ApJ, 381, 200
Yee, H. K. C., Ellingson, E., Bechtold, J., Carlberg, R. G., & Cuilandre, J.-C. 1996, AJ, 111, 1783